Journal of Hazardous Materials 201–202 (2012) 68–73

Contents lists available at SciVerse ScienceDirect

Journal of Hazardous Materials

journal homepage: www.elsevier.com/locate/jhazmat

Heterogeneous Fenton-like catalytic removal of *p*-nitrophenol in water using acid-activated fly ash

Aili Zhang, Nannan Wang, Jiti Zhou*, Ping Jiang, Guangfei Liu

Key Laboratory of Industrial Ecology and Environmental Engineering (Ministry of Education), School of Environmental Science and Technology, Dalian University of Technology, Linggong Road 2, Dalian 116024, PR China

ARTICLE INFO

Article history:
Received 27 April 2011
Received in revised form 6 November 2011
Accepted 8 November 2011
Available online 15 November 2011

Keywords:
Heterogeneous Fenton-like catalysis
Activated fly ash
p-Nitrophenol removal
Leached Fe

ABSTRACT

The use of nitric-acid-activated fly ash (AFA), as heterogeneous Fenton-like catalyst for *p*-nitrophenol (*p*-NP) removal from water, was investigated. The physicochemical characteristics of AFA were better than those of raw fly ash (RFA). Under experimental conditions of pH 1.5–5.1, H_2O_2 dosage 83.3–333 mg L^{-1}, AFA loaded 5.0–20 g L^{-1}, and temperature 298–348 K, the *p*-NP removal rate increased with the increase of H_2O_2 dosage, AFA loaded and temperature. The highest removal rate (98%) was observed at pH 2.0 when H_2O_2 dosage 166.5 mg L^{-1}, AFA loaded 10 g L^{-1} and temperature 298 K. However, good *p*-NP removal efficiency (98.8%) could still be achieved under milder pH (5.1) conditions when enough reaction time (14 h) was applied. The leached iron concentration increased with decrease in pH and with increase in reaction time. The homogenous catalysis caused by leached iron was negligible. The less reaction time and higher AFA load could be selected flexibly for catalytic stability and reusability in actual application. The probable heterogeneous catalytic mechanisms were proposed.

1. Introduction

The treatment of huge amounts of toxic and refractory contaminants in industrial wastewaters has resulted in considerable researches in advanced oxidation processes (AOPs). Especially, Fenton's reagent (i.e., Fe^{2+} and H_2O_2) included in AOPs is more attractive for the effective degradation of pollutants because of its lower cost, lack of toxic reagents and less mass transfer limitation, also its operating conditions are usually mild, hydrogen peroxide is easily handled and the excess of hydrogen peroxide is safe to environment; •OH radicals generated in the Fenton's reagent are well known to be strong oxidants which can destruct many hazardous organic pollutants easily and effectively in wastewater. However, the catalysts (Fe ions) are supplied by adding ferrous salt which make Fenton process have significant disadvantages: (i) in order to achieve satisfied treatment outcome, more ferrous salt should be added, but that will lead to an additional Fe ions pollution in the effluent. (ii) The treatment of the sludge containing Fe ions at the end of the wastewater treatment is expensive in labor, reagents and time. (iii) Fe ions may be deactivated due to the complexation with some iron complexing reagents, such as phosphate anions and intermediate oxidation products [1,2].

Improvement of the homogeneous Fenton or Fenton-like (the use of ferric ions rather than ferrous ions) processes can be achieved by using heterogeneous Fenton-like catalysts. Some heterogeneous catalysts prepared with iron-bearing minerals were used to induce the so-called Fenton-like reaction, which have recently received much attention due to its advantages, such as lower cost, abundance, and environment-friendly nature [3]. Some industrial solid wastes such as kaolin mining [4], pyrite cinder, fly ash [5–8], and steel dust [9,10] were demonstrated to be useful for treatment of various organic pollutants in wastewater when used as heterogeneous Fenton-like catalysts.

Fly ash is a solid waste which is produced from coal-burning power plants or steel mills. It is estimated that over 300 billion tons of fly ash are produced every year in the world [11]. Traditionally, most of fly ash is disposed of through landfill which is causing serious environmental concerns. Recently fly ash has been used as low-cost adsorbent for the removal of pollutants in gaseous and liquids residues [12–14]. Moreover, some studies have demonstrated that fly ash is an interesting heterogeneous catalyst, which could cause catalytic oxidation reactions of H_2S, ethanethiol and methane in exhaust gases [15–17], sodium sulfide in water [18] and esterifiable reactions [11]. However, little information of utilization of acid-activated fly ash (AFA) as catalyst to degrade organic pollutants in water is available.

p-Nitrophenol (*p*-NP) is present in agricultural irrigation effluents [19,20] and industrial effluents discharged from chemical plants producing pesticides, explosives, dyestuffs etc. Due to the

* Corresponding author. Tel.: +86 411 84706252; fax: +86 411 84706252.
E-mail addresses: zjiti@163.com, zal58@163.com (J. Zhou).

0304-3894/$ – see front matter © 2011 Elsevier B.V. All rights reserved.
doi:10.1016/j.jhazmat.2011.11.033

presence of a nitro-group in the aromatic ring [19,20], *p*-NP is toxic, non-biodegradable and highly persistent in the environment, so it has been considered to be priority toxic pollutant by U.S. Environmental Protection Agency (EPA).

In this study, AFA was used as heterogeneous Fenton-like catalyst for the treatment of *p*-NP wastewater. The physicochemical characteristics of AFA, the kinetic performance of *p*-NP removal, the effect of leached iron species and the activity loss were investigated. The probable heterogeneous catalytic mechanisms were suggested by comparing with homogenous catalysis.

2. Materials and methods

2.1. Reagents and fly ash

p-NP (analytical grade) was purchased from Tianjin Kermel Chemical Reagent Co., Ltd., China, and was used as received without further purification. Hydrogen peroxide (30%, w/w) and all other chemicals were of analytical grade if not noted otherwise.

Fly ash was obtained from Donghai Thermal Power Plant in Dalian, China. It was generated from circulating fluidized bed boilers and collected by electrostatic dust catcher. The fly ash was sieved through standard test sieve, then fractions less than 150 μm were used as raw fly ash (RFA) and were further treated by nitric acid. The treatment processes are as follows: 1 g of RFA was mixed with 40 mL of 1 M nitric acid; the mixture was agitated at 25 °C for 4 h and then filtrated. The separated solid was dried at 105 °C and then used as AFA for heterogeneous Fenton-like process.

2.2. Characterization of fly ash samples

1 g of RFA or AFA sample was mixed completely with distilled-deionized water (100 mL) for 10 h. Then the mixture was settled. After that, pH of the supernatant liquor was measured. The chemical compositions of the AFA and RFA samples were determined by X-ray fluorescence spectroscopy (XRF-1800, SHIMADZU). The specific surface area, pore volume and pore size of the samples were measured by BET (Brunauer–Emmett–Teller) automated analyzer (QUADRASORB).

2.3. Wastewater treatment

Firstly, fixed amount of AFA was added in a batch reactor and then unless otherwise specified, 100 mg L^{-1} synthetic *p*-NP solution (100 mL) with predetermined pH value was added. The mixture was homogenized by mechanical agitation. Except for sorption experiments, the reaction started after the addition of a predetermined dosage of H_2O_2. All experiments were carried out in a temperature-controlled water bath and kept constant temperature (±1 °C). At intervals, the mixture was sampled. Before filtration, NaOH solution and MnO_2 were added into the sampled mixture immediately in order to decompose remnant H_2O_2 which can interfere with the measurement of COD. Then the sample was filtrated with vacuum pumping and the filtrate was analyzed to determine *p*-NP concentration, leached amount of irons and chemical oxygen demand (COD). The lifetime of AFA was studied, in this experiment section, the separated solid was dried at 105 °C to constant weight and reused with the same ratio of every reaction ingredient at first run experiment.

2.4. Analytical methods of parameters

The *p*-NP removal efficiency was monitored by measuring the absorbance at 400 nm under pH > 11 (adjusted by adding proper quantities of NaOH) by means of a UV–vis spectrophotometer (JASCO, V-560). The catalyst activity was evaluated by *p*-NP abatement. Oxidation efficiency of H_2O_2 was assessed by the ratio of actual values to theoretical values of COD removal efficiency. COD was determined by using microwave assisted potassium dichromate method [21]. The leached iron was analyzed by flame atomic absorption spectrophotometer (Analyst 700, PerkinElmer Corporation).

The *p*-NP or COD removal efficiency was calculated as:

$$\text{Removal efficiency}\ (\%) = \frac{1 - C_t}{C_0} \times 100 \quad (1)$$

where C_0 and C_t are initial and instantaneous concentrations of *p*-NP or COD (mg L^{-1}).

3. Results and discussion

3.1. Physicochemical characteristics of AFA and RFA

The physicochemical properties of both RFA and AFA samples are shown in Table 1. The major chemical components were SiO_2, CaO, Al_2O_3, Fe_2O_3, LOI and CO_2. The sum of SiO_2, Al_2O_3 and Fe_2O_3 fractions in RFA was greater than 70% indicating that RFA is classified as Type F fly ash according to ASTM C 618. The SiO_2 and Fe_2O_3 contents in AFA were higher than those in RFA, whereas the CaO and Al_2O_3 contents in AFA were smaller. It is well known that low pH value and the exist of Fe ions are important for determining a good efficiency of Fenton reagent [1,5], thus higher Fe_2O_3 contents and lower CaO contents in AFA may be preferred for heterogeneous Fenton-like process. Because of the leaching of alkali metal and metal oxides such as CaO, Al_2O_3 and Fe_2O_3, new smaller pores can be formed on particle surface of RFA, thus the BET area and the total pore volume increased while the average pore diameter decreased when RFA was activated by nitric acid. So compared to RFA, AFA display the higher BET area, the higher total pore volume and the smaller average pore diameter which indicate better adsorption and catalysis capacity. More fractions of larger particle size (105–150 μm) and less fractions of smaller particle size (<105 μm) were found in AFA. Thus the average particle size in AFA was higher than that in RFA indicating better settlement and separation properties.

3.2. Catalytic kinetics of the AFA

As it is well known, pH has significant effect upon the oxidation degradation of organic compounds by hydroxyl radicals in Fenton or Fenton-like reagents [22,23]. As shown in Fig. 1, the *p*-NP removal rate decreased with the sequence of pH 2.0 > 2.5 > 1.5 > 3.0. The 98% *p*-NP removal efficiency was achieved in 40 and 60 min at pH 2.0 and 2.5 respectively. However, only 50% and 12.5% p-NP removal efficiency were achieved in 60 min at pH 1.5 and 3.0 respectively. The tests at milder pH (pH = 5.1) demonstrated that good *p*-NP removal efficiency (98%) could be achieved when enough reaction time (14 h). Due to the highest removal rate of *p*-NP, pH 2.0 was chosen as the optimal pH for further experiments.

Theoretically, 342 mg L^{-1} H_2O_2 is needed to mineralize 100 mg L^{-1} *p*-NP completely according to the stoichiometric Eq. (2):

$$C_6H_5NO_3 + 14H_2O_2 \rightarrow 6CO_2 + 16H_2O + HNO_3 \quad (2)$$

Some researches, such as Fenton, homogeneous Fenton-like [23] and heterogeneous Fenton-like processes using goethite [24] magnetite [25,26] carbon–Fe [1], have shown that the degradation extent of organic compounds was not improved significantly at a higher H_2O_2 dosage because of the competitive reactions of hydroxyl radicals. As higher oxidation efficiency of H_2O_2 was expected, the H_2O_2 effects at lower dosage (25–100% of 342 mg L^{-1}) were investigated. As shown in Fig. 2, the *p*-NP removal rate

Table 1
Comparison of the physical and chemical characteristics of AFA with RFA.

Major chemical component (wt%)						
Sample	SiO_2	CaO	Al_2O_3	Fe_2O_3	[a]LOI	CO_2
AFA	73.6	1.64	8.66	5.73	5.47	2.57
RFA	57.4	10.3	9.76	4.92	8.15	3.57

Other chemical components (wt%)								
Sample	SO_3	MgO	K_2O	P_2O_5	Na_2O	SrO	ZrO_2	ZnO
AFA	1.42	6.9	10.6	1.13	2.93	0.274	0.397	0.0558
RFA	26.9	12.7	8.94	5.44	3.41	1.01	0.331	0.0792

Physical properties				
Sample	BET area ($m^2\ g^{-1}$)	Total pore volume ($\mu L\ g^{-1}$)	Average pore diameter (nm)	[b]pH
AFA	29.99	68.02	9.07	4.19
RFA	11.91	61.65	20.71	9.30

Partial size distribution						
Partial size (μm)		150–125	125–105	105–97	97–88	<88
Sample fractions (wt%)	AFA	19.78	51.69	12.49	1.78	14.27
	RFA	4.03	20.74	33.54	10.10	31.59

[a] The loss on ignition analysis was carried out at 800 °C for 24 h.
[b] 1 g of sample was mixed with 100 mL of distilled-deionized water for 10 h, and the supernatant liquor of the mixture was measured by pH meter.

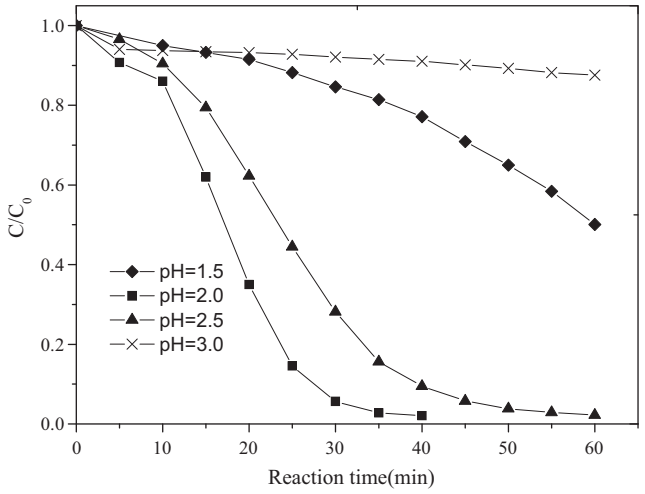

Fig. 1. pH effect on the *p*-NP removal rate. Experimental conditions: initial *p*-NP, 100 mg L^{-1}; initial H_2O_2, 166.5 mg L^{-1}; AFA load, 10 g L^{-1}; temp., 298 K.

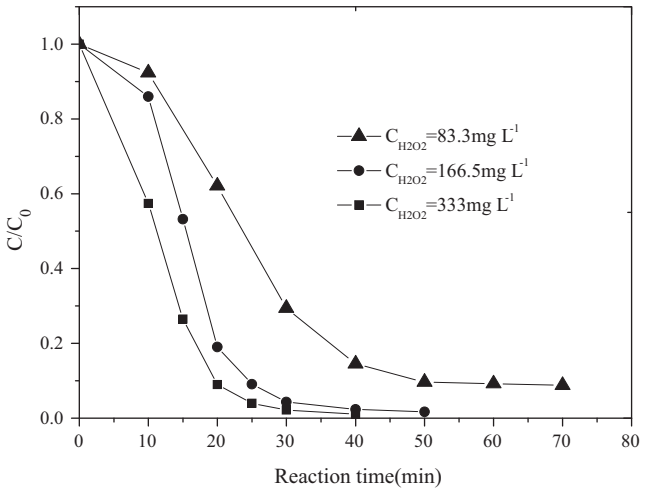

Fig. 2. Effect of H_2O_2 dosages on the *p*-NP removal rate. Experimental conditions: initial *p*-NP, 100 mg L^{-1}; temp., 298 K; AFA load, 10 g L^{-1}; pH = 2.0.

Table 2
COD Removal efficiency and H_2O_2 oxidation efficiency.[a]

Initial H_2O_2 (mg L^{-1})	COD removal efficiency (%)		H_2O_2 oxidation efficiency (%)
	Theoretical values	Actual values	
83.25	25	23	92
166.5	50	48	96
333	100	62	62

[a] Experimental conditions: initial *p*-NP, 100 mg L^{-1}; temp., 298 K; AFA load, 10 g L^{-1}; pH = 2.0; reaction time, 60 min.

increased with increase in H_2O_2 dosage. More than 98% *p*-NP removal efficiencies were achieved in 40 and 50 min for 333 and 166.5 mg L^{-1} H_2O_2 respectively. However, 91% removal efficiency was achieved in 70 min for 83.3 mg L^{-1} H_2O_2.

As shown in Table 2, the highest H_2O_2 oxidation efficiency (the ratio of actual value to theoretical value of COD removal efficiency) was achieved when H_2O_2 dosage is 166.5 mg L^{-1}, this result further indicated the competitive reactions of hydroxyl radicals. Therefore, 166.5 mg L^{-1} H_2O_2 dosage was used in the rest experiments. However, higher dosage of H_2O_2 may be selected in actual application for higher COD removal efficiency.

Generally, Fenton or homogeneous Fenton-like process work well in the presence of small quantities of Fe ions (within 55 mg L^{-1} Fe^{2+} or Fe^{3+}) [23,27,28]. Because of the absence of mass transfer limitation. However, a good heterogeneous Fenton-like process seems to require higher amount of bound iron (about 1.5–3 g L^{-1}) [9,25,29,30]. On the other hand, high iron amount could also act as •OH scavengers [25]. Therefore the appropriate AFA loading of 3.5–20 g L^{-1} (viz. 0.14–0.80 g L^{-1} bound iron according to 5.73 wt% Fe_2O_3 component in AFA) were selected. Preliminary tests demonstrated that *p*-NP could not be removed by H_2O_2 in the absence of the AFA (results not shown) and the *p*-NP removal caused by AFA adsorption was negligible (<0.45 mg g^{-1}). As shown in Fig. 3, the *p*-NP removal rate increased with increase in load of AFA because of the increase in active site for H_2O_2 decomposition and *p*-NP adsorption. The 98% *p*-NP removal efficiency was achieved in 25, 40, 55 and 60 min while 20, 10, 6.5 and 5.0 g L^{-1} AFA was loaded respectively. However, 90% removal efficiency was achieved in 60 min for 3.5 g L^{-1} AFA. Considering lower AFA load and better catalysis performance, 10 g L^{-1} AFA was used in the rest experiments.

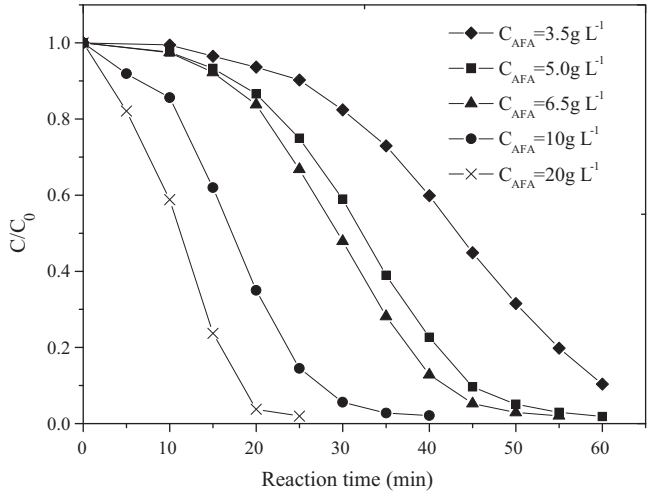

Fig. 3. Effect of AFA load on the *p*-NP removal rate. Experimental conditions: initial *p*-NP, 100 mg L^{-1}; temp., 298 K; pH = 2.0; initial H_2O_2, 166.5 mg L^{-1}.

As shown in Fig. 4, the *p*-NP removal rate increased with increase in temperature indicating that the increase in temperature may be very favorable for increasing number of active surface centers [31]. More than 98% *p*-NP removal efficiency was achieved in 5, 5, 15 and 45 min at 348, 323, 308 and 298 K respectively. However, no significant difference in removal efficiency was observed between 348 and 323 K, This is because of the competition between thermal decomposition of H_2O_2 and free radical formation at higher reaction temperatures [32]. On the other hand, the correlation between temperature and the *p*-NP removal rate may be well explained by Arrhenius equation:

$$\frac{d\ \ln k}{dT} = \frac{E_a}{RT^2} \tag{3}$$

where *T* is reaction temperature, *k* is kinetic reaction rate constant, *R* is gas constant and E_a is the activation energy.

The ln *k* is in inverse ratio with T^2. Consequently, the temperature (323 K) is important for a *p*-NP rapid remove. Considering the efficiency and cost, 298 K was used in the rest experiments.

3.3. Leached iron and concurrent homogeneous catalysis

As shown in Fig. 5, the leached iron concentration increased with decrease in pH and with increase in reaction time. The iron species were also detected simultaneously in the reaction solution (pH 2). As shown in Fig. 6, the concentration of total iron species (Fe^{3+} and Fe^{2+}) in reaction solution increased with increase in reaction time. Here the ascending total iron concentration was most likely

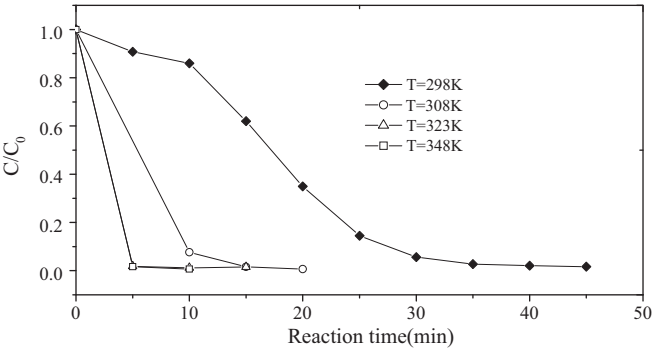

Fig. 4. Effect of temperature on the *p*-NP removal rate. Experimental conditions: initial *p*-NP, 100 mg L^{-1}; pH = 2.0; initial H_2O_2, 166.5 mg L^{-1}. AFA load, 10 g L^{-1}.

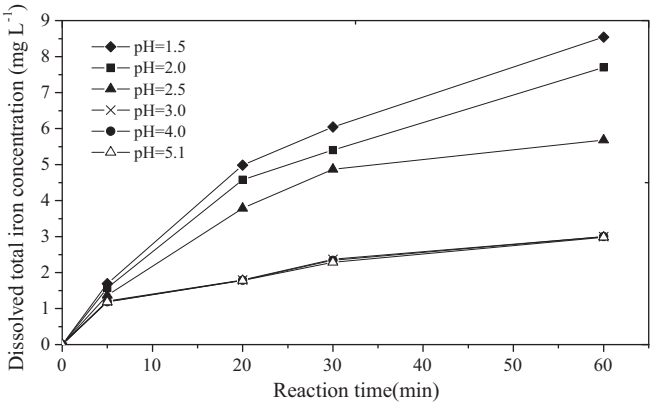

Fig. 5. Effect of pH on leached total iron concentration in the heterogeneous Fenton-like process. Experimental conditions: initial *p*-NP, 100 mg L^{-1}; initial H_2O_2, 166.5 mg L^{-1}; AFA load, 10 g L^{-1}; temp., 298 K.

caused by the gradual oxidation of the surface iron–*p*-NP complexes by H_2O_2, which released ferric ions into solution. The correlation between dissolved total iron and reaction time could be plotted as the quadratic polynomial curve viz. Eq. (4) which showed a good correlation ($R^2 = 0.9975$):

$$C_{dti} = -0.002t^2 + 0.248t \tag{4}$$

where C_{dti} is instantaneous concentrations of dissolved total iron (mg L^{-1}).

As shown in Fig. 6, the curve profiles of $[Fe^{2+}]/[Fe]$ and $[Fe^{3+}]/[Fe]$ were similar to those of the inter-conversion of ferric ions and ferrous ions during homogeneous Fenton-like [33]. These results suggested that ferric ions were first leached from AFA and then a part of ferric ions was converted to ferrous ions by H_2O_2 until the maximum amount of ferrous ions was obtained in 18 min. After that, ferrous ions were converted by H_2O_2 to ferric ions again.

Because of the leached Fe ions, the heterogeneous Fenton-like process and homogeneous Fenton-like process must proceed simultaneously. The occurrence time of maximum concentration of ferrous ion is close to the starting time of the highest removal rate of *p*-NP (see also Fig. 1). Therefore hydrogen peroxide was catalyzed by both iron species bound to the surface of AFA (heterogeneous reaction) and aqueous iron species (homogenous reaction).

In order to understand the contribution of homogeneous Fenton-like process to the *p*-NP removal efficiency, a controlled experiment was carried out, in which homogeneous ferric ion (Fe^{3+}) was used as catalyst instead of AFA and was added gradually into the reaction solution at different reaction time. The concentrations

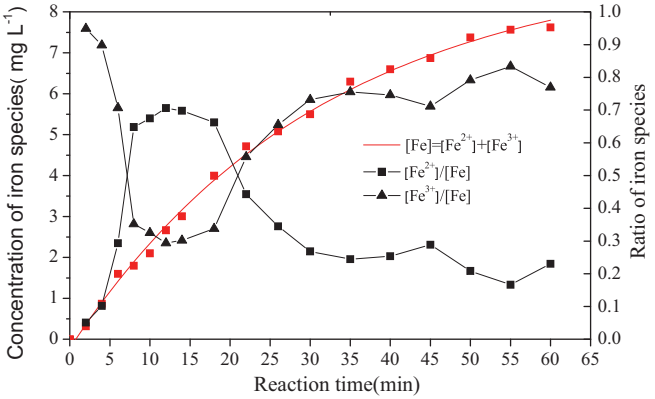

Fig. 6. Concentration of leached iron species and ratio of ferric or ferrous ion to total iron ion versus reaction time. Experimental conditions: initial *p*-NP, 100 mg L^{-1}; initial H_2O_2, 166.5 mg L^{-1}; AFA load, 10 g L^{-1}; temp., 298 K, pH 2.0.

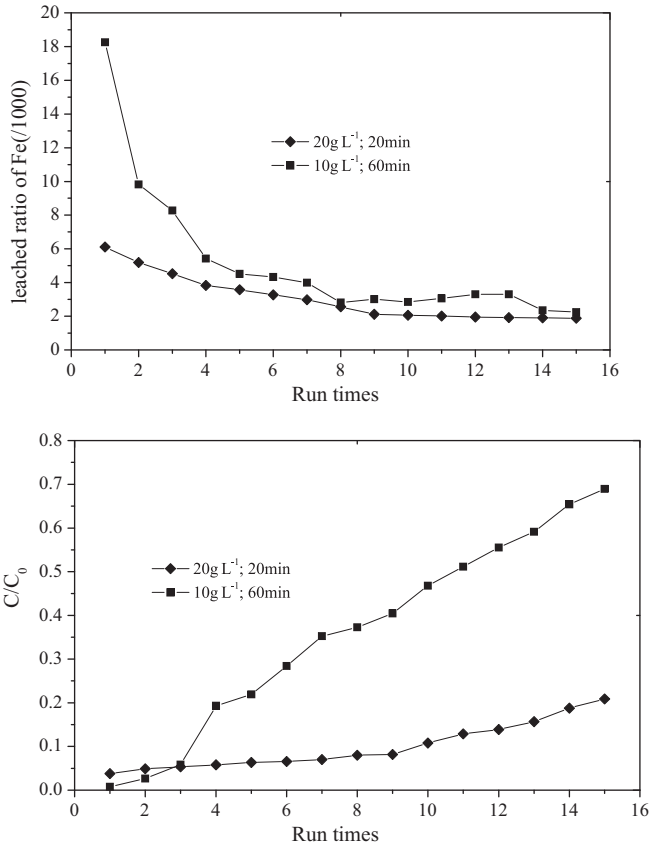

Fig. 7. Catalytic activity loss and leached ratios of Fe in reutilization of AFA. Experimental conditions: initial *p*-NP, 100 mg L^{-1}; pH = 2.0; initial H_2O_2, 166.5 mg L^{-1}; T = 298 K.

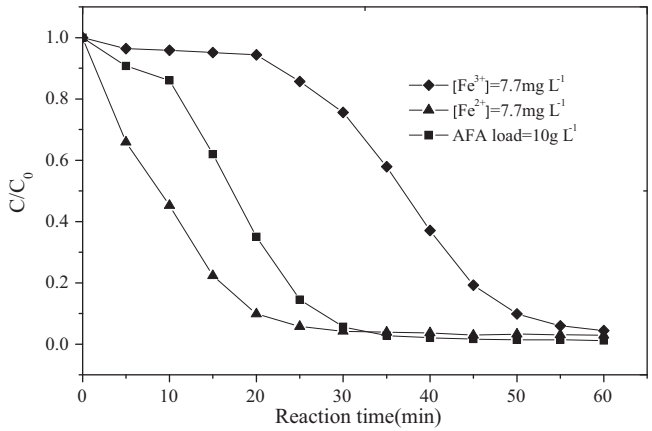

Fig. 8. The *p*-NP removal rates under different catalyst. Experimental conditions: initial *p*-NP, 100 mg L^{-1}; pH = 2.0; initial H_2O_2, 166.5 mg L^{-1}; T = 298 K.

of ferric ion added at different reaction time were calculated based on Eq. (4). The *p*-NP removal efficiency increased slowly with increase in reaction time and was only 2.79% in 30 min, which was far less than that (94.4% in 30 min from Fig. 1) of heterogeneous Fenton-like process. Therefore concurrent homogeneous Fenton-like reactions played negligible role in the *p*-NP removal.

3.4. The loss of AFA catalytic activity

From the view of actual application, catalytic stability and reusability are very important. Two AFA re-utilization experiments (re-exp.) were carried out in the same pH and H_2O_2 dosage but varied reaction time and AFA load. The re-exp. 1 was conducted using 10 g L^{-1} AFA for 60 min and the re-exp. 2 was conducted using 20 g L^{-1} AFA for 20 min. During the reaction cycles, as shown in Fig. 7, the decrease of both *p*-NP removal efficiency and the ratio of leached Fe were faster in re-exp. 1 indicating that the loss of AFA catalytic activity was due to the loss of Fe irons in catalyst. Hence, less reaction time and higher AFA load may be selected in actual application for catalytic stability and reusability.

3.5. AFA catalytic mechanisms

Catalytic kinetics of the AFA at pH < 3 exhibited a two-phase removal rate of *p*-NP, viz. an initial slow removal phase and then a rapid one (Figs. 1–4). Although similar results have been observed previously, little was known about the detailed mechanisms [23,34–36]. Some researches suggested that the existence of initial slow removal period was due to the requiring time for surface activation, whereas some related it to the reactant adsorption onto the catalyst surface [34]. Also some researches explained the heterogeneous Fenton-like catalysis by analogous reactions to the homogeneous Fe^{3+} catalysis [25,37]. To explain AFA catalytic mechanisms, two experiments based on homogeneous iron (Fe^{3+} and Fe^{2+}) catalysis were carried out at pH 2 respectively: based on the concentration of leached Fe ions (7.7 mg L^{-1}) in 60 min in AFA catalytic system, instead of AFA, 7.7 mg L^{-1} Fe^{2+} ions or Fe^{3+} ions was added into reaction system to initiate homogeneous reaction. The *p*-NP removal rates were compared among the three kinds of catalyst (AFA, Fe^{3+} and Fe^{2+}) (Fig. 8). The curve profile of *p*-NP removal rate using AFA was similar to that using 7.7 mg L^{-1} Fe^{3+}, i.e. an initial slow removal rate was followed by a rapid removal rate of *p*-NP. However, when 7.7 mg L^{-1} Fe^{2+} was applied, a rapid removal rate of *p*-NP was observed from the beginning and was maintained until 90% p-NP was removed in 20 min. Therefore the probable heterogeneous catalytic mechanisms were proposed by comparing with the decomposition of H_2O_2 by homogeneous Fe^{3+} (Table 3). An initial reaction chain (reactions (1)–(3b)) probably occurred on and near the iron-bearing surface sites in AFA, the $\equiv Fe^{III}$–hydroperoxy complexes were formed (the symbol "≡" represents the iron species bound to the surface of AFA), and their unimolecular decomposition yielded $\equiv Fe^{II}$ and hydroperoxy/superoxide radicals ($HO_2\bullet/O_2\bullet^-$). According to the rate constants of reactions (3a) and (3b), $\equiv Fe^{III}$ was converted slowly to $\equiv Fe^{II}$. It is well known that oxidation potential of reactive oxygen species ($HO_2\bullet$ and $O_2\bullet^-$) is much smaller than that of the HO• species, thus a slow *p*-NP removal period appeared initially. Afterward, as the reaction continues, the reaction 4 probably occurred on and near the iron-bearing surface sites. On the other hand, the interactions between *p*-NP and surface sites (SS) could be described as equilibrium reaction between sorbed and aqueous species:

$$SS + p\text{-}NP_e \rightarrow SS(p\text{-}NP)_s \quad (5)$$

The HO• radicals formed by reaction (4) could attack the sorbed species as well as the aqueous species, which led to the degradation

Table 3
Mechanisms of H_2O_2 decomposition by homogeneous Fe^{3+} [33].

No.	Reactions	Rate constants
1	$Fe^{3+} + H_2O_2 \leftrightarrows Fe^{III}(HO_2)^{2+} + H^+$	$k_1 = 3.1 \times 10^{-3}$
2	$FeOH^{2+} + H_2O_2 \leftrightarrows Fe^{III}(OH)(HO_2)^+ + H^+$	$k_2 = 2.0 \times 10^{-4}$
3a	$Fe^{III}(HO_2)^{2+} \rightarrow Fe^{2+} + HO_2\bullet$	$k_{3a} = 2.7 \times 10^{-3}\ s^{-1}$
3b	$Fe^{III}(OH)(HO_2)^+ \rightarrow Fe^{2+} + HO_2\bullet/O_2\bullet^- + OH^-$	$k_{3b} = 2.7 \times 10^{-3}\ s^{-1}$
4	$Fe^{2+} + H_2O_2 \rightarrow Fe^{3+} + HO\bullet + OH^-$	$k_4 = 63.0\ M^{-1}\ s^{-1}$
5	$Fe^{2+} + HO\bullet \rightarrow Fe^{3+} + OH^-$	$k_5 = 3.2 \times 10^8\ M^{-1}\ s^{-1}$
6	$H_2O_2 + HO\bullet \rightarrow HO_2\bullet + H_2O$	$k_6 = 3.3 \times 10^7\ M^{-1}\ s^{-1}$
7	$HO\bullet + HO\bullet \rightarrow H_2O_2$	$k_7 = 5.2 \times 10^9\ M^{-1}\ s^{-1}$
8	$HO\bullet + RH \rightarrow \bullet R + H_2O$	$k_8 = 10^7 - 10^{10}\ M^{-1}\ s^{-1}$

and mineralization of *p*-NP:

$$HO + SS(p\text{-NP})_s \rightarrow SS + (p\text{-NPby-products})_{solution} \rightarrow NO_3{}^- + CO_2 \quad (6)$$

$$HO + p\text{-NP}_e \rightarrow p\text{-NPby-products} \rightarrow NO_3{}^- + CO_2 \quad (7)$$

According to rate constant of reaction (4), $\equiv Fe^{II}$ was converted rapidly to $\equiv Fe^{III}$. In addition, it is well known that oxidation potential of HO• radicals is very high (2.80), thus a rapid *p*-NP removal period appeared. According to chemical reaction equilibrium, the decrease in pH value could cause the increase in reaction rate of (3b)–(5). The reason that *p*-NP removal rate at pH 2 was higher than that at pH 2.5 might be attributed to reaction (3b) and (4). The lower removal rate of *p*-NP at pH 1.5 might be due to two reasons: first, the more leached Fe decreased the iron-bearing surface sites; second, the quenching function of reaction (5) toward HO•. At pH 3.0–5.1, the much slower removal rate of *p*-NP might be attributed to the formation of $HO_2\bullet/O_2\bullet^-$ with smaller oxidation potential yielded by reactions (3a) and (3b) while without formation of appreciable amount of hydroxyl radicals.

There were shortened trend of initial slow removal period with increase in H_2O_2 dosages (Fig. 2), AFA load (Fig. 3) and temperature (Fig. 4), indicating that the rates of reactions (1)–(3b) increased with increase in H_2O_2 dosages, AFA load and temperature.

4. Conclusions

The chemical components, physical properties (BET area, total pore volume, average pore diameter and pH) and particle size distribution of AFA as heterogeneous Fenton-like catalyst were better than those of RFA. Under experimental conditions of pH 1.5–5.1, H_2O_2 dosage 83.3–333 mg L^{-1}, AFA loaded 5.0–20 g L^{-1} and temperature 298–348 K, the *p*-NP removal rate increased with the increase in H_2O_2 dosage, AFA loaded and temperature, and was fastest at pH 2.0. However H_2O_2 oxidation efficiency was highest (96%) under 166 mg L^{-1} H_2O_2 dosage and good *p*-NP removal efficiency (98.8%) can be achieved under milder pH (5.1) when enough reaction time (14 h) was applied. The leached iron concentration increased with decrease in pH and with increase in reaction time. The homogenous catalysis of leached iron for *p*-NP removal was negligible. The less reaction time and higher AFA load should be selected for catalytic stability and reusability in actual application. The probable heterogeneous catalytic mechanisms could be proposed by comparing with the decomposition of H_2O_2 by homogeneous Fe^{3+}.

References

[1] J.H. Ramirez, F.J. Maldonado-Hodar, A.F. Perez-Cadenas, C. Moreno-Castilla, C.A. Costa, L.M. Madeira, Azo-dye Orange II degradation by heterogeneous Fenton-like reaction using carbon–Fe catalysts, Appl. Catal. B 75 (2007) 312–323.

[2] J.H. Deng, J.Y. Jiang, Y.Y. Zhang, X.P. Lin, C.M. Du, Y. Xiong, $FeVO_4$ as a highly active heterogeneous Fenton-like catalyst towards the degradation of Orange II, Appl. Catal. B 84 (2008) 468–473.

[3] E.G. Garrido-Ramirez, B.K.G. Theng, M.L. Mora, Clays and oxide minerals as catalysts and nanocatalysts in Fenton-like reactions – a review, Appl. Clay Sci. 47 (2010) 182–192.

[4] M.C. Pereira, C.M. Tavares, J.D. Fabris, R.M. Lago, E. Murad, P.S. Criscuolo, Characterization of a tropical soil and a waste from kaolin mining and their suitability as heterogeneous catalysts for Fenton and Fenton-like reactions, Clay Miner. 42 (2007) 299–306.

[5] Y. Flores, R. Flores, A.A. Gallegos, Heterogeneous catalysis in the Fenton-type system reactive black 5/H_2O_2, J. Mol. Catal. A: Chem. 281 (2008) 184–191.

[6] Y.L. Song, J.T. Li, Degradation of CI Direct Black 168 from aqueous solution by fly ash/H_2O_2 combining ultrasound, Ultrason. Sonochem. 16 (2009) 440–444.

[7] L. Yi, Z. Fu-Shen, Catalytic oxidation of methyl orange by an amorphous FeOOH catalyst developed from a high iron-containing fly ash, Chem. Eng. J. 158 (2010) 148–153.

[8] H. Liu, M.Y. Liang, C.S. Liu, Y.X. Gao, J.M. Zhou, Catalytic degradation of phenol in sonolysis by coal ash and H_2O_2/O^{3-}, Chem. Eng. J. 153 (2009) 131–137.

[9] J.M. Lee, J.H. Kim, Y.Y. Chang, Y.S. Chang, Steel dust catalysis for Fenton-like oxidation of polychlorinated dibenzo-p-dioxins, J. Hazard. Mater. 163 (2009) 222–230.

[10] R. Mecozzi, L. Di Palma, D. Pilone, L. Cerboni, Use of EAF dust as heterogeneous catalyst in Fenton oxidation of PCP contaminated wastewaters, J. Hazard. Mater. 137 (2006) 886–892.

[11] C. Khatri, A. Rani, Synthesis of a nano-crystalline solid acid catalyst from fly ash and its catalytic performance, Fuel 87 (2008) 2886–2892.

[12] M. Ahmaruzzaman, Role of fly ash in the removal of organic pollutants from wastewater, Energy Fuels 23 (2009) 1494–1511.

[13] S.B. Wang, H.W. Wu, Environmental-benign utilisation of fly ash as low-cost adsorbents, J. Hazard. Mater. 136 (2006) 482–501.

[14] S.H. Chang, K.S. Wang, H.C. Li, M.Y. Wey, J.D. Chou, Enhancement of rhodamine B removal by low-cost fly ash sorption with Fenton pre-oxidation, J. Hazard. Mater. 172 (2009) 1131–1136.

[15] J.R. Kastner, K.C. Das, Q. Buquoi, N.D. Melear, Low temperature catalytic oxidation of hydrogen sulfide and methanethiol using wood and coal fly ash, Environ. Sci. Technol. 37 (2003) 2568–2574.

[16] E.V. Fomenko, E.V. Kondratenko, A.N. Salanov, O.A. Bajukov, A.A. Talyshev, N.G. Maksimov, V.A. Nizov, A.G. Anshits, Novel microdesign of oxidation catalysts. Part 1. Glass crystal microspheres as new catalysts for the oxidative conversion of methane, Catal. Today 42 (1998) 267–272.

[17] P. Kolar, J.R. Kastner, J. Miller, Low temperature catalytic oxidation of aldehydes using wood fly ash and molecular oxygen, Appl. Catal. B 76 (2007) 203–217.

[18] D. Mallick, S. Khanra, S.K. Chaudhuri, Studies on the potential of coal fly ash as a heterogeneous catalyst in oxidation of aqueous sodium sulfide solutions with hydrogen peroxide, J. Chem. Technol. Biotechnol. 70 (1997) 231–240.

[19] Z.I. Bhatti, H. Toda, K. Furukawa, p-Nitrophenol degradation by activated sludge attached on nonwovens, Water Res. 36 (2002) 1135–1142.

[20] M.C. Tomei, M.C. Annesini, R. Luberti, G. Cento, A. Senia, Kinetics of 4-nitrophenol biodegradation in a sequencing batch reactor, Water Res. 37 (2003) 3803–3814.

[21] D.M. Dharmadhikari, A.P. Vanerkar, N.M. Barhate, Chemical oxygen demand using closed microwave digestion system, Environ. Sci. Technol. 39 (2005) 6198–6201.

[22] T. Zhou, Y.Z. Li, J. Ji, F.S. Wong, X.H. Lu, Oxidation of 4-chlorophenol in a heterogeneous zero valent iron/H_2O_2 Fenton-like system: kinetic, pathway and effect factors, Sep. Purif. Technol. 62 (2008) 551–558.

[23] C.C. Jiang, S.Y. Pang, F. Ouyang, J. Ma, J. Jiang, A new insight into Fenton and Fenton-like processes for water treatment, J. Hazard. Mater. 174 (2010) 813–817.

[24] J.J. Wu, M. Muruganandham, J.S. Yang, S.S. Lin, Oxidation of DMSO on goethite catalyst in the presence of H_2O_2 at neutral pH, Catal. Commun. 7 (2006) 901–906.

[25] X.F. Xue, K. Hanna, M. Abdelmoula, N.S. Deng, Adsorption and oxidation of PCP on the surface of magnetite: kinetic experiments and spectroscopic investigations, Appl. Catal. B 89 (2009) 432–440.

[26] X.F. Xue, K. Hanna, N.S. Deng, Fenton-like oxidation of rhodamine B in the presence of two types of iron (II, III) oxide, J. Hazard. Mater. 166 (2009) 407–414.

[27] X.R. Xu, H.B. Li, W.H. Wang, J.D. Gu, Degradation of dyes in aqueous solutions by the Fenton process, Chemosphere 57 (2004) 595–600.

[28] J.A. Zazo, J.A. Casas, A.F. Mohedano, J.J. Rodriguez, Semicontinuous Fenton oxidation of phenol in aqueous solution. A kinetic study, Water Res. 43 (2009) 4063–4069.

[29] R.M. Liou, S.H. Chen, M.Y. Hung, C.S. Hsu, J.Y. Lai, Fe (III) supported on resin as effective catalyst for the heterogeneous oxidation of phenol in aqueous solution, Chemosphere 59 (2005) 117–125.

[30] M. Muruganandham, J.S. Yang, J.J. Wu, Effect of ultrasonic irradiation on the catalytic activity and stability of goethite catalyst in the presence of H_2O_2 at acidic medium, Ind. Eng. Chem. Res. 46 (2007) 691–698.

[31] Q. Zhang, W.F. Jiang, H.L. Wang, M.D. Chen, Oxidative degradation of dinitro butyl phenol (DNBP) utilizing hydrogen peroxide and solar light over a Al_2O_3-supported Fe(III)-5-sulfosalicylic acid (ssal) catalyst, J. Hazard. Mater. 176 (2010) 1058–1064.

[32] G.B.O. de la Plata, O.M. Alfano, A.E. Cassano, Decomposition of 2-chlorophenol employing goethite as Fenton catalyst. I. Proposal of a feasible, combined reaction scheme of heterogeneous and homogeneous reactions, Appl. Catal. B 95 (2010) 1–13.

[33] J. De Laat, H. Gallard, Catalytic decomposition of hydrogen peroxide by Fe(III) in homogeneous aqueous solution: mechanism and kinetic modeling, Environ. Sci. Technol. 33 (1999) 2726–2732.

[34] M.L. Luo, D. Bowden, P. Brimblecombe, Catalytic property of Fe–Al pillared clay for fenton oxidation of phenol by H_2O_2, Appl. Catal. B 85 (2009) 201–206.

[35] M.N. Timofeeva, S.T. Khankhasaeva, S.V. Badmaeva, A.L. Chuvilin, E.B. Burgina, A.B. Ayupov, V.N. Panchenko, A.V. Kulikova, Synthesis, characterization and catalytic application for wet oxidation of phenol of iron-containing clays, Appl. Catal. B 59 (2005) 243–248.

[36] E. Guelou, J. Barrault, J. Fournier, J.M. Tatibouet, Active iron species in the catalytic wet peroxide oxidation of phenol over pillared clays containing iron, Appl. Catal. B 44 (2003) 1–8.

[37] R. Matta, K. Hanna, S. Chiron, Fenton-like oxidation of 2,4,6-trinitrotoluene using different iron minerals, Sci. Total Environ. 385 (2007) 242–251.